Mechanistic Aspects of Mechanically Induced Phase Transformations

F. DELOGU[1], G. MULAS[2], S. ENZO[2], L. SCHIFFINI[2] and G. COCCO[2]

[1]*Dipartimento di Ingegneria Chimica e Materiali, Universita degli Studi di Cagliari, Piazza d'Armi, I-09123 Cagliari (Italy)*

E-mail: delogu@dicm.unica.it

[2]*Dipartimento di Chimica, Universita degli Studi di Sassari, Via Vienna 2, I-07100 Sassari (Italy)*

Abstract

In the field of mechanochemistry, the exact nature of the atomistic processes underlying physical and chemical transformations under mechanical processing conditions is a long-standing problem. Far from being satisfactorily solved, the lively debate associated has constantly stimulated the development of conceptual frameworks alternative to the defect-enhanced thermal diffusion scenarios initially proposed. Different approaches laying emphasis on the capability of mechanical forces to induce atomic scale mixing phenomena independent of thermal contribution were thus investigated. Along this line of inquiry, molecular dynamics simulations were here employed to gain deeper insight into the atomic-scale processes induced at the phase boundary between crystalline Ni and Zr metal lattices by the application of a shear stress. The numerical findings show that the application of shear stresses determines the deformation of the crystal and the formation of a sliding interface. Atoms with defective coordination appear at the interfacial region and gradually arrange into complex aggregates, the dynamics of which promotes the migration of atomic species and their gradual mixing near the interface. Chemical disordering processes take place at the interface, resulting in the formation of an amorphous domain.

INTRODUCTION

It is well known that the plastic deformation of a crystalline solid takes place *via* the formation and interaction of point, line and plane defects [1–3]. The storage of excess potential energy due to the accumulation of local atomic strains enhances the chemical reactivity [1–3], thus favouring the occurrence of phase transformations [4–6]. These processes underlie the modern mechanochemical methods, based on the repeated mechanical loading of powder particles trapped between colliding surfaces and the related occurrence of local shear events on the microscopic scale [6–8]. Under such circumstances, the large amounts of energy localized in relatively small volumes of a solid promote anomalously fast local processes of mass transport and mixing [9–21], which then cannot be related to thermal diffusion scenarios [22–27]. The present work aims to investigate the effect of localized mechanical stresses on the atomistic behaviour by focusing on the early stages of the deformation processes taking place when two semi-crystals of different metals undergo shearing and collision events. To this end, molecular dynamics simulations were used as detailed in the following.

COMPUTATIONAL OUTLINE

Calculations were carried out on Ni and Zr semicrystals. Shearing and collision events were simulated by applying a combination of normal and tangential forces. In the case of shearing events, the system consisted of 18000 Ni atoms arranged in a stacking sequence of 20 [111] *fcc* cF4 planes and 18750 Zr atoms arranged in a stacking sequence of 30 [100] *hcp* hP2 planes. A smooth interface between Ni and

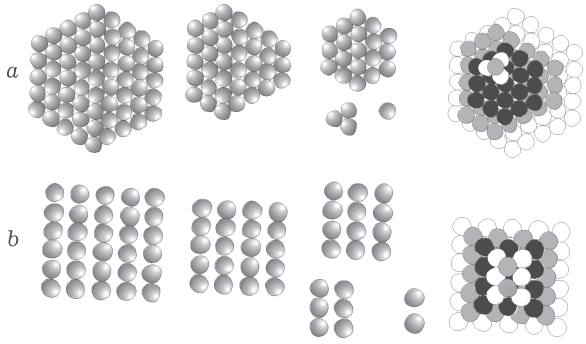

Fig. 1. Schematic depiction of the structural motifs (right) and their simple components (left) employed to model the surface of the Ni (*a*) and of the Zr (*b*) semicrystals.

Zr semi-crystals was created by approaching the two lattices along the *z* Cartesian direction up to the distance of the minimum enthalpy. Collision events were indeed studied by employing semicrystals with a rough surface. The Ni semicrystal was prepared by starting from 17100 atoms arranged in a stacking sequence of 19 (111) planes. The surface morphology was arbitrarily defined by randomly placing on the surface four assemblies of 120 atoms identical to the one schematically depicted in Fig. 1, *a*. The Ni semicrystal was therefore formed by 17580 atoms. The Zr semicrystal was prepared by starting from 18125 atoms arranged in a stacking of 29 (100) planes. The surface structure was modeled by randomly placing on the surface three assemblies of 70 atoms identical to the one schematically illustrated in Fig. 1, *b*. The Zr semicrystal contained then 18335 atoms. The Ni semicrystal was placed above the Zr one along the *z* Cartesian direction at a distance of 0.4 nm. The number of atoms per side of the semicrystals was selected to minimize the mismatch effects due to the different atomic sizes.

Interactions, described by a semi-empirical many-body tight-binding force scheme based on the second-moment approximation to the electronic density of states [28–30], were computed within a cutoff radius approximately corresponding to the seventh shell of neighbors in Ni [28–31]. The potential parameter values were taken from literature [28, 29]. The equations of motion were solved by employing a fifth-order predictor-corrector algorithm [32] with a time step δt equal to 2.0 fs.

Periodic boundary conditions were applied along the *x* and *y* Cartesian directions, whereas a "reservoir region" of seven atomic planes was defined along the *z* Cartesian direction at one end of each semicrystal, the free surface being located at the opposite end. Within each reservoir, the five atomic planes more distant from the free surface consisted of immobile atoms occupying ideal lattice positions. The Nosè-Hoover thermostat [33] was applied to keep the temperature *T* constant at 300 K and the Parrinello–Rahman scheme was implemented to deal with eventual shape changes of the elementary crystallographic cells [34]. The single Ni and Zr semicrystals were separately relaxed at 300 K for 1 ns. Tangential and/or normal external constant forces were applied to reservoir regions after the equilibration stage. In the case of shearing, a tangential force (F_t) was applied along the *x* Cartesian direction to simulate a shear stress and obtain a couple of sliding. Correspondingly, opposite centre-of-mass

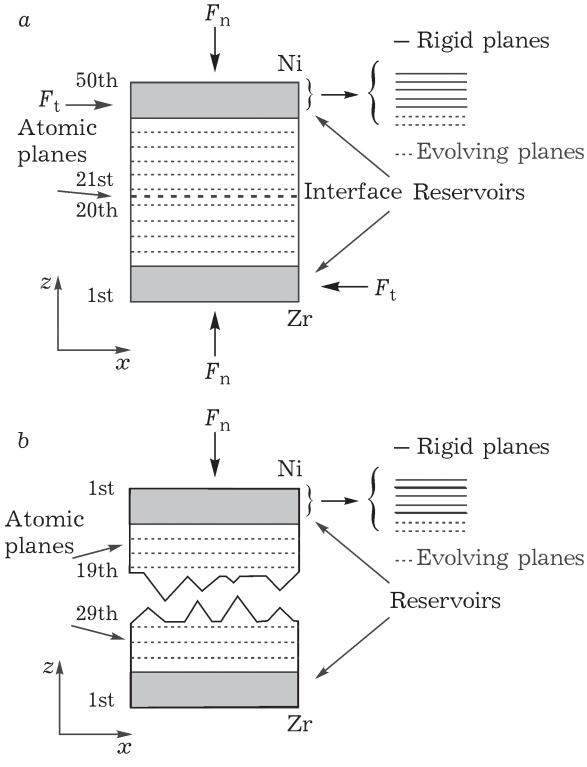

Fig. 2. Schematic illustration of the simulated systems: *a* – the system configuration employed to simulate a shearing event, *b* – the systems configuration employed to simulate a collision between rough surfaces. The normal and tangential forces F_n and F_t are indicated.

velocities of about 10 m/s were given to the Ni and Zr systems [10]. A weak normal force (F_n) was here applied to reservoirs to keep them at a roughly constant distance along the z Cartesian direction. The simulation time (t) was scaled to 0 when the combination of forces was applied. In the case of collision, a normal force F_n was applied to reservoirs to give a centre-of-mass velocity along the z Cartesian direction of about 10 m/s [10]. The impact event began when a couple of Ni and Zr atoms approached to a distance smaller than the equilibrium distance between Ni and Zr atoms at 0 K. In this case, the simulation time t was scaled to 0 at the beginning of the collision event. A schematic illustration of the systems investigated is shown in Fig. 2.

The degree of crystalline order was quantified by means of the planar static order parameter $S_p(\boldsymbol{k})$ [32]. $S_p(\boldsymbol{k})$ was evaluated with reference to the (111) and (100) crystallographic planes for Ni and Zr respectively. The three-dimensional static order parameter $S(\boldsymbol{k})$ and the pair correlation function (PCF) $g(r)$ were also used [32]. The rearrangement of atomic positions due to local shearing events was followed by looking at the atoms characterized by a coordination number different from 12. Two atoms were regarded as nearest neighbours when located at distances smaller than the one, r_m, corresponding to the first minimum in the PCF of the region considered.

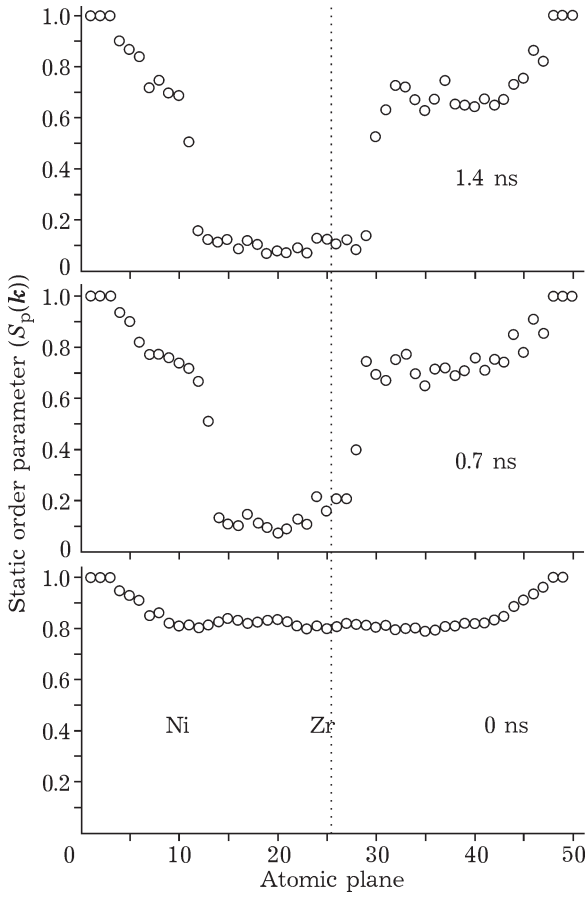

Fig. 3. Planar structure factor $S_p(\boldsymbol{k})$ for the different atomic planes at the simulation times quoted. As evident from the PCF $g(r)$ quoted in the inset, the interfacial region amorphizes.

SHEARING EVENT

The application of tangential forces determines the slow relative motion of atomic planes, which produces plastic deformation and then structural defects. The first pairs of atoms with coordination numbers equal to 11 and 13 seem to be randomly distributed. Such apparent randomness is gradually lost as the number of defective atom pairs increases, the underlying mechanism of defective atom formation possessing a cooperative character. The planar static order parameter $S_p(\boldsymbol{k})$ values, quoted in Fig. 3 at different times, gradually decrease due to disordering phenomena progressively involving all the system. The relatively complex dynamics of defective atoms is also responsible for the gradual intermixing of atomic species, which in turn determines a gradual loss of structural order. The collapse of the crystalline lattices and the formation of an amorphous layer involves however only the interfacial region, as also shown by the PCF of the region between the 14th and 27th planes after 0.7 ns reported in the inset of Fig. 3. The thickness Δ of the perturbed, intermixed layer increases with time. A rough estimate of the intermixed layer thickness Δ can be obtained as the difference between the z Cartesian coordinates of the Ni and Zr atoms closest respectively to the Zr and Ni reservoir regions. As shown in Fig. 4, Δ^2 scales linearly with the square root of the time. This suggests that shear-induced mixing and thermal diffusion processes could have deep analogies. Shear-induced mixing is mediated by apparently random processes involving small clusters of at-

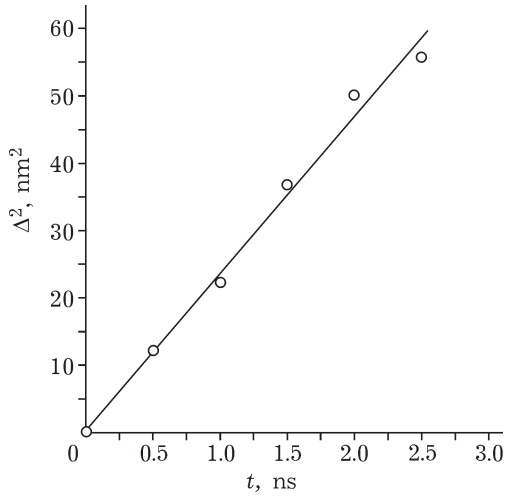

Fig. 4. Square of the mixed layer thickness (Δ^2) as a function of time (t).

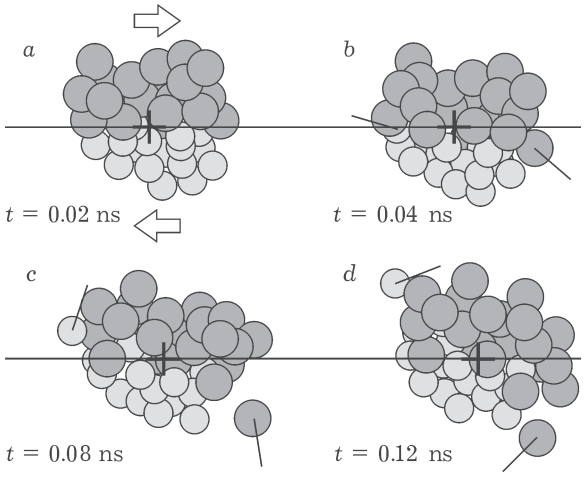

Fig. 5. Snapshots of an atomic cluster, formed by 21 Ni (light grey) and 26 Zr (heavy grey) atoms strongly interacting, undergoing a slow rotation at the times quoted. Large arrows in (*a*) indicate the sense of sliding, *i.e.* of cluster rotation. Small sections indicate the displacement direction of single atoms. The dotted horizontal line represents the original position of interface, while the cross represents the approximate position of the centre of rotation.

oms characterized by relatively high mobility. Such clusters slowly rotate around axes along the y Cartesian direction, with single atoms randomly leaving and joining the cluster as shown in Fig. 5. The apparent diffusion coefficient amounts to about $2 \cdot 10^{-8}$ m^2/s and is orders of magnitude larger than the one pertaining to thermal processes.

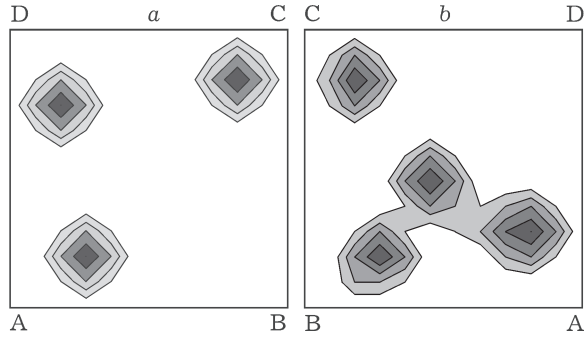

Fig. 6. Projection of the surface structure on the (x;y) plane for the Zr (*a*) the Ni (*b*) semicrystals. A density level map is reported. The Ni and Zr semicrystals in the simulation cell are reciprocally oriented in order that the letters superpose.

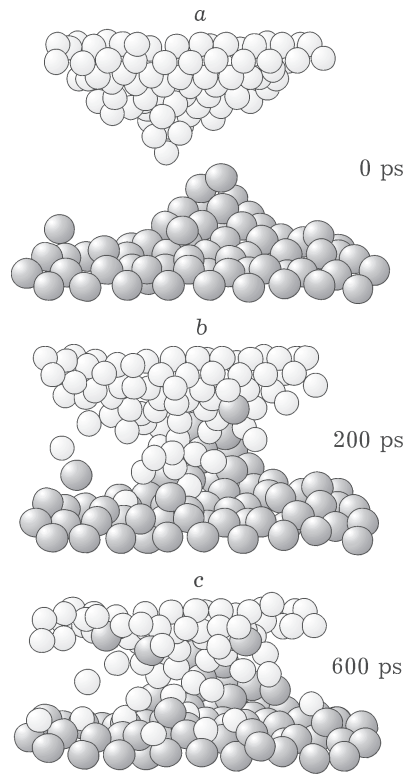

Fig. 7. Atomic configurations of two colliding assemblies at the Ni and Zr surfaces at the times quoted. Atomic species at the surface are heavily displaced from their positions by the action of local shear stresses.

COLLISION EVENT

The impact between the (111) Ni surface with four asperities and the (100) Zr surface with three asperities is the case study of collisions between anomalously rough surfaces. The patterns shown in Fig. 6 indicate that two Ni asperities are located approximately in coinci-

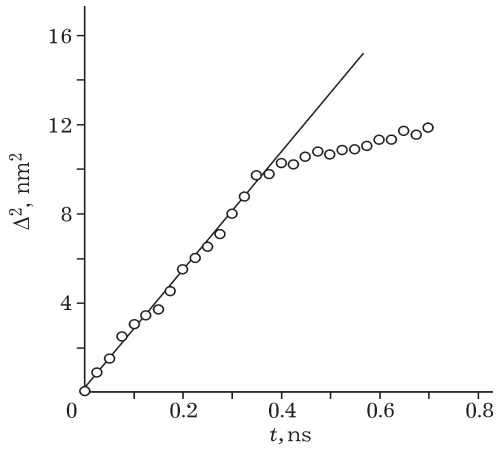

Fig. 8. Square of the thickness of the mixed layer (Δ^2) as a function of the time (t). Two approximately linear regimes are evident.

dence with two Zr asperities. These represent then the points of first contact between the Ni and Zr semicrystals. The intense mechanical loads developing at such points give rise to shear stresses inducing ballistic atomic displacement conditions, as pointed out by the snapshots of atomic configurations reported in Fig. 7. An increase in the kinetic energy of surface atoms and then in local temperatures T, which attain values as high as 2100 K, is accompanied by a rapid mixing of atomic species in quasi-molten regions. The planar static order parameter $S_p(\boldsymbol{k})$ values indicate that the mechanical deformation gradually propagates below the surfaces along the z Cartesian direction at a rate of about 100 m/s. Defective atoms appear in correspondence with the asperities and successively spread over more extended regions, attaining a more uniform distribution. They form irregular clusters undergoing a continuous change of size and position. A certain number of closed loops of defective atoms are seen to approximately correspond to Shockley partial dislocations with gliding systems characteristics of *fcc* and *hcp* lattices. The large surface roughness determines rapid mixing phenomena and the formation of a mixed layer of thickness Δ. The plot of Δ^2 as a function of t, reported in Fig. 8, points out two dynamical regimes. Initially Δ displays a time dependence analogous to the one pertaining to conventional thermal diffusion. A definite slope decrease is however observed after about 0.35 ns, due to the strong interaction between the surface asperities with either each other or the surface of the opposite semicrystal after about 0.3 ns. At times longer than 0.35 ns the two semicrystals experience thus an intense compressive load that induces a change of the atomic rearrangement mechanism from ballistic conditions to less energetic ones. This results in turn in a decrease of the rate with which the amorphous layer grows.

CONCLUSIONS

The evidences hitherto discussed suggest that mixing and amorphization processes are governed by local shear-induced atomic displacements. The application of mechanical forces at relatively low temperature determines a complex sequence of atomic-scale processes, propagating from the surface to the interior of semicrystals and inducing the interfacial mixing of chemical species. Significant atomic position rearrangements take place *via* the formation of atoms with defective coordination. Local shear events are responsible for the interfacial mixing of elements and the formation of a layer of intermixed species. Its thickness increases with time according to a power law similar to the one characteristic of thermal diffusion. In this case, however, atomic displacements are solely due to shear events. Shear-induced mixing processes display then deep analogies with thermal diffusion, although on a different time scale. Far from being exhaustive, the numerical findings point out the important role played by the shear-induced displacements of atomic species in the formation of a disordered interface.

Acknowledgements

Financial support has been provided by the University of Sassari and the University of Cagliari. A. Ermini, ExtraInformatica s.r.l., is gratefully acknowledged for the technical support.

REFERENCES

1 Physical Metallurgy, 4th Ed., in R. W. Cahn and P. Haasen (Eds.), Elsevier Science BV, Amsterdam, 1996.
2 K. E. Easterling and D. A. Porter, Phase Transformations in Metals and Alloys, 2nd Ed., Chapman & Hall, London, UK, 1992.
3 C. Kittel, Introduction to Solid State Physics, 7th Ed., J. Wiley & Sons, New York, 1996.

4 G. Heinicke, Tribochemistry, Akademie-Verlag, Berlin, 1984.
5 P. Yu. Butyagin, *Sov. Sci. Rev. B Chem.*, 14 (1989) 1.
6 C. Suryanarayana, *Prog. Mat. Sci.*, 46 (2001) 1.
7 B. B. Khina, F. H. Froes, *J. Met.*, 48 (1996) 36.
8 T. H. Courtney, *Mat. Trans., JIM*, 36 (1995) 110.
9 P. Bellon, R. S. Averback, *Phys. Rev. Lett.*, 74 (1995) 1819.
10 J. E. Hammerberg, B. L. Holian, J. Roder *et al.*, *Physica D*, 123 (1998) 330.
11 R. G. Hoagland, M. I. Baskes, *Scripta Mat.*, 39 (1998) 417.
12 V. Bulatov, F. F. Abraham, L. Kubin *et al.*, *Nature*, 391 (1998) 669.
13 I. A. Ovid'ko, A. B. Reizis, *J. Phys. D: Appl. Phys.*, 32 (1999) 2833.
14 X. Y. Fu, M. L. Falk, D. A. Rigney, *Wear*, 250 (2001) 420.
15 M. F. Horstemeyer, M. I. Baskes, S. J. Plimpton, *Acta Mat.*, 49 (2001) 4363.
16 K. Kadau, T. C. Germann, P. S. Lomdahl, B. L. Holian, *Science*, 296 (2002) 1681.
17 A. C. Lund, C. A. Schuh, *Appl. Phys. Lett.*, 82 (2003) 2017.
18 V. I. Levitas, *Phys. Rev. B*, 70 (2004) 184118.
19 F. Delogu, G. Cocco, *Ibid.*, 71 (2005) 144108.
20 F. Delogu, G. Cocco, *Ibid.*, 72 (2005) 014124.
21 F. Delogu, G. Cocco, *Ibid.*, 2006, in press.
22 W.L. Johnson, *Prog. Mat. Sci.*, 30 (1986) 81.
23 W. J. Meng, C. W. Nieh, W. L. Johnson, *Appl. Phys. Lett.*, 51 (1987) 1693.
24 U. Gosele, K. N. Tu, *J. Appl. Phys.*, 66 (1989) 2619.
25 R. J. Highmore, *Phil. Mag. B*, 62 (1990) 455.
26 L. Greer, *Ibid.*, 61 (1990) 525.
27 R. Yavari, P. J. Desrи, *Mat. Sci. Forum*, 88–90 (1992) 43.
28 C. Massobrio, V. Pontikis, G. Martin, *Phys. Rev B*, 41 (1990) 10486.
29 V. Rosato, M. Guillope, B. Legrand, *Phil. Mag. A*, 59 (1989) 321.
30 F. Ducastelle, *J. Phys.* (Paris), 31 (1970) 1055.
31 P. Mura, P. Demontis, G. B. Suffritti *et al.*, *Phys. Rev. B*, 50 (1994) 2850.
32 M. P. Allen and D. Tildesley, Computer Simulation of Liquids, Clarendon Press, Oxford, UK, 1987.
33 S. Nosč, *J. Chem. Phys.*, 81 (1984) 511.
34 M. Parrinello, A. Rahman, *J. Appl. Phys.*, 52 (1981) 7182.